

Anomalous x-ray diffraction of an hexagonal Fe/Ru superlattice

M. De Santis,* A. De Andres,[†] and D. Raoux[‡]

Laboratoire pour l'Utilisation du Rayonnement Electromagnétique, Bâtiment 209 d, 91405 Orsay, France

M. Maurer,[§] M. F. Ravet,** and M. Piecuch

Laboratoire Mixte, CNRS, Saint Gobain, Boîte Postale 109, 54709 Pont-à-Mousson, France

(Received 30 March 1992)

Molecular-beam-epitaxy-grown hexagonal Fe/Ru superlattices have been investigated by anomalous x-ray diffraction near the iron absorption K edge to inquire selectively into the structure of both the iron and the ruthenium sublattices. The data have been analyzed by comparing simulated and experimental spectra in k space at various wavelengths and by means of a difference Fourier-transform method that allows us to trace the iron density profile along the growth direction of the superlattice and then directly probe the Fe/Ru interface. From both methods we extract the interplanar spacing for Fe and Ru. We get $c_{\text{Fe}} \sim 4.11 \text{ \AA}$ and $c_{\text{Ru}} \sim 4.33 \text{ \AA}$. The value $a \sim 2.69 \text{ \AA}$ is the same for both sublattices. We can thus calculate the atomic volume of hexagonal Fe in the superlattice $V_{\text{Fe}} \sim 12.87 \text{ \AA}^3$ which is expanded by 14% with respect to hcp Fe. This may explain the onset of ferromagnetism in this metastable hexagonal Fe phase.

INTRODUCTION

The advances in deposition techniques have made possible the sequential layer-by-layer growth of several kinds of materials. This capability has been extensively exploited to build nearly flawless semiconductor superlattices. Recently an increasing interest has been devoted to the molecular-beam-epitaxy (MBE) growth of metallic superlattices.^{1,2} The efforts in this direction are driven by several possible technological applications like optics for soft x ray and magneto-optic data recording.

Despite the large lattice mismatch, Fe/Ru superlattices have been prepared by MBE.³ Previous work has shown that the iron layers have an expanded metastable hexagonal structure, which is pseudomorphous with hcp Ru.³ Frank-Van der Merve growth is observed up to about seven Fe monolayers. Theoretical calculations using the local spin-density approximation show that the iron atomic volume is a very critical parameter for the stability of an iron ferromagnetic phase. The hexagonal hcp phase which can be stabilized under pressure is not magnetic, though calculations show it would become magnetic if the atomic volume would be increased significantly.⁴ Experimentally Fe_x/Ru_y superlattices show no sign of localized magnetism for $x \leq 8 \text{ \AA}$. Above this threshold (four Fe planes per period) the magnetic moment increases linearly with the Fe thickness, the moment being about $2 \mu_B$ per Fe atom.⁵ It is known that hcp $\text{Fe}_x/\text{Ru}_{1-x}$ solid solutions show no stable magnetic moment up to a Fe concentration as high as $x = 75\%$. The presence of Ru atoms reduces the exchange interactions thus destroying the magnetism. Interdiffusion at the Fe/Ru interfaces could thus explain the existence of two magnetically dead planes at each interface. Even though the Fe hexagonal structure in Fe/Ru superlattice has already been established, a more accurate insight into local structure, lattice constants, and interlayer

interdiffusion is needed to explain the magnetic behavior and the metastability of the hexagonal Fe phase. In this paper we use anomalous x-ray diffraction which is a unique tool to selectively probe the two different kinds of sublattices. Two different samples have been investigated, one being nonmagnetic (Fe_4/Ru_4) and the other one having two magnetically ordered planes ($\text{Fe}_{12}/\text{Ru}_{16}$).

I. EXPERIMENT

The samples were grown by MBE on a (1120) sapphire substrate, on top of a 200- \AA -thick (0001) Ru buffer layer.³ Reflection high-energy electron diffraction (RHEED) streaks ensured that the surface remains flat and single crystalline all along the growth. Auger spectroscopy did not reveal significant interdiffusion. X-ray diffraction on powdered samples suggests a hcp-like structure. Rocking curves are smooth with a full width at half maximum of about 1° both in the layer plane and along the growth direction.

The anomalous x-ray-diffraction experiments have been carried out at LURE using a two circle diffractometer. The scattering plane is vertical in order to use efficiently the linear polarization of the beam. A Si (220) double crystal monochromator already described in Ref. 9 was used. The diffraction spectra were measured both in the transmission geometry with $\mathbf{k} \perp c$ to find the in-plane lattice constant a , and in the symmetric reflection geometry, i.e., with $\mathbf{k} \parallel c$ in a k range spanning from 0.1 to 6.3 \AA^{-1} and with a high- k resolution of about $5 \times 10^{-3} \text{ \AA}^{-1}$ due mainly to the slit width. This resolution allows us to partially resolve the contribution from the Ru buffer from the multilayer peaks as shown in Fig. 1. Spectra in reflection geometry were collected at various energies, 6539, 7112, 8333, and 15203 eV for a $\text{Fe}_{12}/\text{Ru}_{16}$ sample with 70 bilayers, each one made of nominally $n_{\text{Fe}} = 6$ and $n_{\text{Ru}} = 8$ planes, and at 7112, 7709,

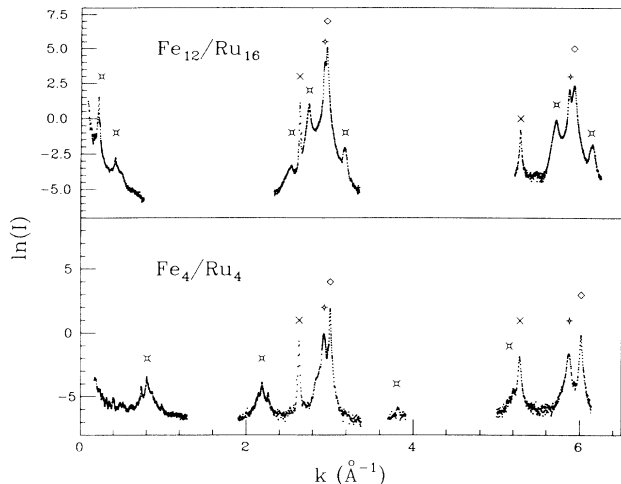


FIG. 1. Upper panel: diffracted intensity of a $\text{Fe}_{12}/\text{Ru}_{16}$ superlattice measured at 8333 eV (logarithmic scale); lower panel: diffracted intensity of a Fe_4/Ru_4 superlattice at 7709 eV. \diamond , (0002 n) superlattice Bragg peaks; \square , satellites; $+$, Bragg peaks of Ru buffer; \times , sapphire substrate.

8979, and 15 203 eV for a sample Fe_4/Ru_4 ($n_{\text{Fe}} = n_{\text{Ru}} = 2$, 100 bilayers). The related variations in the iron (and ruthenium) scattering and absorption factors which are listed in Table I have been taken from Ref. 6 except at 7112 eV. For that energy close to the Fe-K absorption edge, f'_{Fe} has been measured from x-ray-absorption data and f''_{Fe} calculated using the Kramers-Kronig relation.

In Fig. 1, one of the measured spectra for each sample (at 8333 eV for $\text{Fe}_{12}/\text{Ru}_{16}$ and at 7709 eV for Fe_4/Ru_4) has been plotted (in logarithmic scale). These spectra have already been corrected for geometrical factors like the angular dependence of the diffracting volume, absorption effects which strongly depend on the photon energy, as well as shifts in k space due to the refraction index. The spectra at different energies have been normalized one with respect to the others by using the intensities of the reflections from the Ru buffer.

Data examination for the $\text{Fe}_{12}/\text{Ru}_{16}$ sample shows the following gross trends: First, the (0002) and (0004) Bragg peaks of the hexagonal superlattice cell are incompletely resolved from those of the Ru buffer layer due to the difference between the values of the c parameter of the buffer and of the mean c value of the superlattice. Second, we observe several satellites due to the multilayer stacking. We get two satellites at small angles and one satellite on each side of each Bragg peak of the mean lat-

TABLE I. Anomalous corrections to the atomic scattering factors (in electron units, Ref. 6). The values f'_{Fe} and f''_{Fe} at the iron edge (*) have been calculated from extended x-ray-absorption fine-structure measurements (Ref. 7).

| E (eV) | 6539 | 7112 | 7709 | 8333 | 8979 | 15 203 |
|-------------------|--------|--------|--------|--------|--------|--------|
| f'_{Fe} | -2.325 | -7.5* | -1.726 | -0.894 | -0.44 | 0.298 |
| f''_{Fe} | 0.541 | 1.0* | 3.425 | 3.033 | 2.678 | 1.097 |
| f'_{Ru} | -0.032 | -0.037 | -0.077 | -0.141 | -0.223 | -1.084 |
| f''_{Ru} | 4.659 | 4.053 | 3.553 | 3.112 | 2.726 | 1.084 |

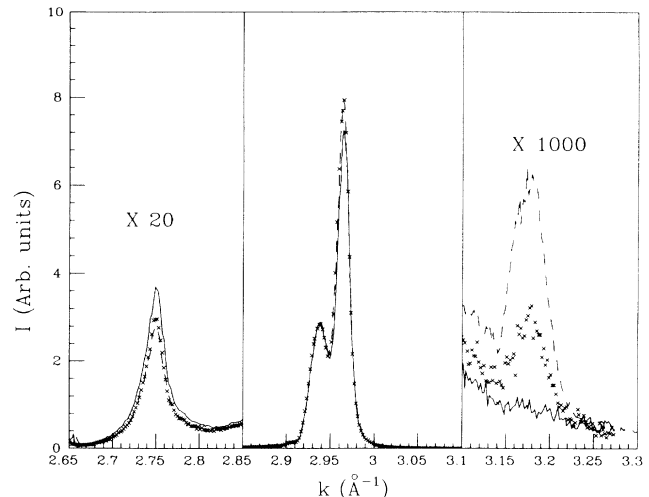


FIG. 2. Experimental spectra of the $\text{Fe}_{12}/\text{Ru}_{16}$ superlattice in the region of the (0002) Bragg peak and of its satellites. The spectra at 6539 eV (crosses), 7112 eV (full line), and 8333 eV (dashed line) are shown. The satellite on the low- k side is amplified by a factor 20 and the one at higher k by a factor 1000.

tice. The intensity of the low- k satellite is much larger than that of the weak high- k satellite. This directly indicates a larger $c/2$ interplanar distance for the Ru sublattice, the Ru atoms having a stronger scattering factor. Another very weak satellite can be seen on the low- k side at two times the Bragg peak to first satellite distance but its intensity is too weak to be registered with accuracy. Third, the widths of the satellites are larger than those of the Bragg peaks of the mean hexagonal cell. Nevertheless, an increase with k values of the widths both for Bragg peaks and satellites is observed. Finally, the intensity dependence versus the Fe scattering factor $f_{\text{Fe}}(E, k)$ is moderately positive for the main Bragg peaks (0002 and 0004), very large for the high- k satellites at $+2\pi/\Lambda$ and negative for the low- k satellites at $-2\pi/\Lambda$, Λ being the wavelength of the modulation (Fig. 2).

The Fe_4/Ru_4 sample can be actually considered as a regular single crystal with a period along the c axis of about 8 Å. However, the first peak as well as the other satellites have a complex shape. Moreover, the satellite positions show that the number of planes for each iron-ruthenium bilayer is not an integer.

II. k -SPACE ANALYSIS

In the kinematic approximation the diffracted intensity with a scattering vector \mathbf{k} parallel to the c axis is given by

$$I(E, k) \propto \left| \sum_j f_j(E, k) \exp(iz_j k) \right|^2, \quad (1)$$

where $f_j(E, k) = f_j^0(k) + f_j'(E) + i f_j''(E)$ and z_j are, respectively, the scattering amplitude of atom j and its position along the c axis. For a periodic structure, $I(E, k)$ can be written as the product $|S(k)|^2 |F(E, k)|^2$ where $F(E, k)$ is the structure factor of the supercell of size Λ , and $S(k)$ is the Fourier transform of the modulation at a

period Λ . For an ideal superlattice, assuming the same in-plane atomic density for Ru and Fe, we have

$$F(E, k) = f_{\text{Fe}} \frac{\sin(n_{\text{Fe}} d_{\text{Fe}} k / 2)}{\sin(d_{\text{Fe}} k / 2)} + f_{\text{Ru}} \exp(ik \Lambda / 2) \frac{\sin(n_{\text{Ru}} d_{\text{Ru}} k / 2)}{\sin(d_{\text{Ru}} k / 2)}, \quad (2)$$

where d_{Fe} (d_{Ru}) is the interplanar distance between Fe (Ru) planes and $\Lambda = n_{\text{Fe}} d_{\text{Fe}} + n_{\text{Ru}} d_{\text{Ru}}$ is the period of the superlattice. For a perfect stacking of N bilayers, the $S(k)$ factor is given by $\sin(N\Lambda k / 2) / \sin(\Lambda k / 2)$; it is energy independent and for samples having a large number of periods N , it is a series of δ -like functions peaking at $2\pi p / \Lambda$, where p is an integer number (see Fig. 3). Actually, in order to simulate $I(E, k)$ for real samples, we have to take into account both microscopic and "macroscopic" defects, such as steps and terraces, different orientations or different sizes of domains, fluctuations of the Λ period over the sample, interlayer diffusion, fluctuation in the number of Fe or Ru planes, interfacial roughness, etc. To reach a good agreement between calculations and experimental spectra is a difficult task since all these defects do contribute. We show how anomalous x-ray diffraction data can be exploited in a very simple framework to eliminate the influence of many of these parameters. Let us consider the integrated intensities for each diffraction peak at $k = k_i$ and for each energy E_j . For thick samples with large N values the ratio of the integrated intensities calculated at two different energies for the same peak depends only on the supercell structure factors,

$$\frac{I(E_j, k_i)}{I(E_l, k_i)} = \frac{\int_{\Delta k_i} |S(k) F(E_j, k)|^2 dk}{\int_{\Delta k_i} |S(k) F(E_l, k)|^2 dk} \approx \frac{|F(E_j, k_i)|^2}{|F(E_l, k_i)|^2}. \quad (3)$$

$$|F(E, k)| = \left| \frac{\sin(p\pi n_{\text{Fe}} / n)}{\sin(p\pi / n)} \frac{1 + dkn_{\text{Fe}} n_{\text{Ru}} \cotg(p\pi n_{\text{Fe}} / n) \epsilon / 2n}{1 + (n_{\text{Ru}} - n_{\text{Fe}}) \cotg(p\pi / n) dk \epsilon / 2n + n_{\text{Fe}} n_{\text{Ru}} [\cotg(p\pi / n) dk \epsilon / 2n]^2} \times [\Delta f - f \cotg(p\pi / n) dk \epsilon / 2] \right|. \quad (4)$$

In this formula only the last term in square brackets is energy dependent. For reasonably small ϵ values the anomalous effect is expected to be strong for small p satellite indexes and for a large number n of planes (i.e., large period Λ). This is what is experimentally found for the $\text{Fe}_{12}/\text{Ru}_{16}$ sample. Conversely, it also explains why the scattered intensity for Fe_4/Ru_4 is not so sensitive to Δf variations.

We have focused on the (0002) $\text{Fe}_{12}/\text{Ru}_{16}$ main Bragg peak, its low- k satellite (at $-2\pi/\Lambda$) and its high- k satellite (at $+2\pi/\Lambda$) which exhibit the largest anomalous

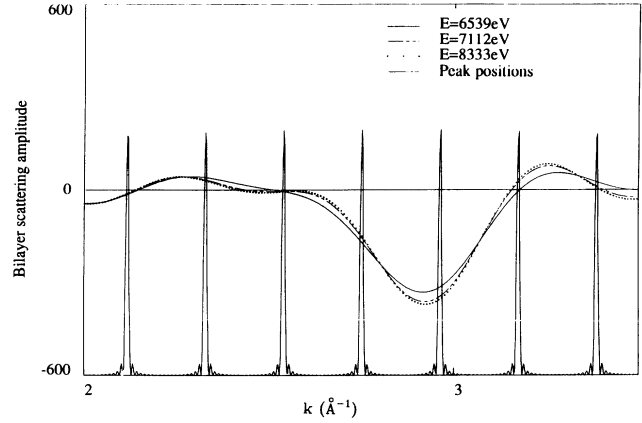


FIG. 3. The supercell scattering amplitude $F(E, k)$ in the region $2 \text{ \AA}^{-1} < k < 3.5 \text{ \AA}^{-1}$ calculated for $E = 7112, 6539,$ and 8333 eV with $d_{\text{Ru}} = 2.17 \text{ \AA}$ and $d_{\text{Fe}} = 2.05 \text{ \AA}$. The delta-like features represent $|S(k)|^2$ (calculated for a superlattice with 30 bilayers) and show the peak positions.

This ratio eliminates overall factors which are not energy dependent, like the Debye-Waller factor $\exp(-\sigma^2 k^2)$. It is thus, to a large extent, insensitive to the defects which reduce the diffracted intensities. This is the main advantage of using anomalous diffraction.

The formula (2) can be rewritten as a function of the average values of the scattering factor f , of the average interplanar distance d , and of the reduced parameters $\Delta f / f$ and $\epsilon = \Delta d / d$, where $f = (n_{\text{Fe}} f_{\text{Fe}} + n_{\text{Ru}} f_{\text{Ru}}) / n$, $n = n_{\text{Fe}} + n_{\text{Ru}}$, $d = (n_{\text{Fe}} d_{\text{Fe}} + n_{\text{Ru}} d_{\text{Ru}}) / n$, $\Delta f = f_{\text{Ru}} - f_{\text{Fe}}$, and $\Delta d = d_{\text{Ru}} - d_{\text{Fe}}$. To understand the energy dependence of the intensities, we can perform a first-order expansion in ϵ since it is expected to be small. This yields a simple result for the structure factor of the p th satellite of a (000 m) Bragg peak of the mean lattice located at $k = 2\pi m / d + 2\pi p / \Lambda$,

layer is given by

$$n = n_{\text{Ru}} + n_{\text{Fe}} = \frac{\Lambda}{d} = \Lambda \times \frac{k_{\text{Bragg}}}{2\pi}, \quad (6)$$

where k_{Bragg} is the wave vector of the (0002) Bragg peak. In our case, n is found to be equal to the nominal total number of planes (14) in the limit of the experimental inaccuracy. In Fig. 4 the ratios of the intensities calculated from (3) to the measured ones are plotted as function of c_{Fe} . Actually, in Fig. 4, we have plotted the ratio of the intensities calculated for two different energies divided by the ratio of the measured ones. This eliminates the first two terms in (4) which are not energy dependent and allows an accurate measurement of $\varepsilon = \Delta d/d$, the other parameters in the energy-dependent term in square brackets being already determined. This allows us to determine c_{Fe} . We have plotted $A = I(7112, k_2)/I(8333, k_2)$, $B = I(6539, k_2)/I(8333, k_2)$, and $C = I(8333, k_1)/I(7112, k_1)$ ($k_2 = 3.175 \text{ \AA}^{-1}$ and $k_1 = 2.75 \text{ \AA}^{-1}$). The fourth plot is the ratio $D = I(8333, k_2)/I(8333, k_1)$, which also depends on the relative value of c_{Fe} and c_{Ru} . For each curve the agreement between theoretical and experimental data should occur for intensity ratios equal to one. We find that this occurs for the same ε value, though we have an error bar on the experimental data shown in Fig. 4 due mainly to the normalization by the intensity scattered by the Ru buffer peaks and to the background subtraction which is important to accurately measure the intensity of the weak high- k satellite. The insufficient stability of the monochromator during the whole measurement could also bring an uncertainty to the f'_{Fe} value at 7112 eV which we estimate to be at most equal to 0.5 in electronic units, corresponding to a shift of less than 0.005 \AA in line A. The theoretical calculation of the intensity $I(E_j, k_2)$ of the satellite at $k_2 = 3.175$

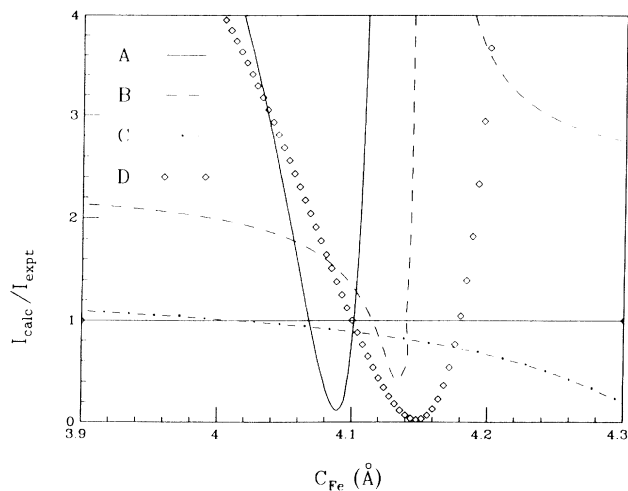


FIG. 4. Dependence of the intensities of the satellites versus the c lattice parameter. The intensities calculated for a perfect superlattice have been divided by the experimentally determined ones to yield relative intensities $I(E, k)$. $A = I(7112, k_2)/I(8333, k_2)$; $B = I(6539, k_2)/I(8333, k_2)$; $C = I(8333, k_1)/I(7112, k_1)$; and $D = I(8333, k_2)/I(8333, k_1)$ ($k_2 = 3.175 \text{ \AA}^{-1}$, $k_1 = 2.75 \text{ \AA}^{-1}$, and the energies are in eV).

\AA^{-1} is affected slightly by the number N of periods [i.e., by the width of $S(k)$] because the $S(k)$ peak falls near a zero of $F(E, k)$. We see in Fig. 4 that all the lines approximately cross 1 for $c_{\text{Fe}} \sim 4.11 \pm 0.01 \text{ \AA}$. From this value of c_{Fe} we find using (5) $c_{\text{Ru}} \sim 4.33 \pm 0.01 \text{ \AA}$. In order to test how the results depend on $n_{\text{Ru}} - n_{\text{Fe}}$ we have performed the same calculation with $n_{\text{Ru}} = 7$ and $n_{\text{Fe}} = 7$. All the plots shift by about 0.01 \AA towards higher c_{Fe} values.

These results are not so much model dependent as could be thought at first view. If we consider, for example, the extended step model⁸ taking into account a Gaussian distribution of the number of planes or/and of the interatomic distances at the interface between the two metals, the analytic expressions for the intensity ratios A , B , and C are exactly the same, provided the widths of the distributions are the same for the iron and the ruthenium layers.

We have seen that for the $\text{Fe}_{12}/\text{Ru}_{16}$ superlattice the mean number of atomic planes in each bilayer $n_{\text{Ru}} + n_{\text{Fe}}$ is an integer as expected. The situation is found to be different for the short period superlattice Fe_4/Ru_4 . In this case the first Bragg peak occurs at $k_{\text{Bragg}} = 3.004 \text{ \AA}^{-1}$, which corresponds to a mean interplanar distance of 2.091 \AA . Its satellite peaks at 2.194 \AA^{-1} , i.e., at 0.810 \AA^{-1} from the maximum of the Bragg peak. In good agreement, the first peak at low angles is found at 0.811 \AA^{-1} (Fig. 1). From both measurements, we get the same $\Lambda = 7.750 \pm 0.005 \text{ \AA}$ value. This value gives us a period [see Eq. (6)] of about 3.7 planes for each bilayer instead of the nominal four planes for each.

To find the iron atomic volume, we have also measured the diffraction spectra in the transmission mode, for the $\text{Fe}_{12}/\text{Ru}_{16}$ sample, with the k vector parallel to $(1\bar{1}00)$. The measurements have been performed at $15\,250 \text{ eV}$ to reduce the x-ray absorption from the thick sapphire substrate. The measurements have been taken for the $(1\bar{1}00)$, $(2\bar{2}00)$, and $(3\bar{3}00)$ Bragg peaks and for the three equivalent directions in the (a, b) hexagonal plane. We have found in each spectrum a double peak, with a rocking curve which is roughly one degree. The splitting is larger for the $(3\bar{3}00)$ reflection which has been used for quantitative measurements. The first peak of the doublet at $k = 8.040 \text{ \AA}^{-1}$ corresponds quite well to the $(3\bar{3}00)$ Bragg peak of bulk ruthenium ($a = 2.7058$, i.e., $k = 8.044 \text{ \AA}^{-1}$) and is due to the Ru buffer. The second one at $k = 8.090 \text{ \AA}^{-1}$ has been assigned to the superlattice and yields a shorter lattice constant: $a_{\text{Fe}/\text{Ru}} = 2.689 \text{ \AA}$. No other peaks have been detected confirming a commensurate epitaxy between iron and ruthenium layers. For the ruthenium in the superlattice, the increase in the c parameter from 4.2811 \AA (bulk value) to 4.33 \AA compensates the decrease in the a parameter ($\Delta a/a = -6 \times 10^{-3}$) induced by epitaxy so that its atomic volume is almost the same as in bulk ruthenium ($\Delta V/V \sim -9 \times 10^{-4}$). We can also calculate the atomic volume for iron in the $\text{Fe}_{12}/\text{Ru}_{16}$ superlattice: $V_{\text{Fe}} = (\frac{3}{4})^{1/2} a_{\text{Fe}/\text{Ru}}^2 c_{\text{Fe}} = 12.87 \text{ \AA}^3$. This high value of the atomic volume may explain why the iron atoms carry a high magnetic moment⁵ in the superlattice, while they are not magnetic in the regular compact hcp phase.

At last we want to point out that, while the hexagonal symmetry is well established, further studies are needed to test the hcp stacking. The diffraction x-ray measurements in transmission mode show an anomaly in the diffracted intensity of the (2200) superlattice Bragg peak when compared to the (1100) and (3300) peaks. The (2200) peak has a lower intensity than the expected one for a hcp lattice. This could indicate a deviation from the hcp stacking which has also been suggested by an x-ray absorption study.⁷ However, until now our trials to measure the diffraction peaks forbidden in a hcp packing have been unsuccessful, so that the actual structure of the hexagonal Fe sublattice is still puzzling.

III. FOURIER-TRANSFORM METHOD

From a diffraction pattern, it is possible to obtain directly the electronic density in real space by means of a Fourier transform (FT) of the scattered amplitude. This implies the phasing of the reflections. Thus we can get the electronic density across the multilayer by Fourier transforming the amplitude scattered with the scattering vector perpendicular to the stacking. To do this, we need to know the phases for all the reflections. We can see the supercell of an ideal superlattice as a sandwich of n_B atomic planes B between two layers of $n_A/2$ atomic planes A . Such a superlattice is therefore a centrosymmetric crystal. The phases of the scattered amplitudes are thus real and equal to ± 1 . We have calculated them for a perfect $\text{Fe}_{12}/\text{Ru}_{16}$ multilayer and assumed that they are correct for the actual sample, which turns out to be reasonable as discussed hereafter.

Indeed we can write the scattered amplitude A of the real crystal as a sum of the perfect multilayer scattering amplitude A_{perf} (which is real) and of a deviation $\Delta A = A - A_{\text{perf}} = \Delta A' + i\Delta A''$ which may be complex. Assuming that $|\Delta A| \ll A_{\text{perf}}$, we get $|A| = [(A_{\text{perf}} + \Delta A')^2 + (\Delta A'')^2]^{1/2} \sim |A_{\text{perf}} + \Delta A'|$ to the first order. Assuming the phase to be real, we indeed calculate the Fourier transform of $A_{\text{perf}} + \Delta A' = (A + A^*)/2$. This operation is equivalent to symmetrizing the Fe/Ru and the Ru/Fe interfaces. It exactly provides the physical information we are looking for, because it gives information on the average defects on the two interfaces. Now we consider the effect of a possible interdiffusion at the interfaces on the phase sign. The supercell scattering amplitude is a slowly varying k function and it is of order of f_i except for well identified and narrow k domains where its sign changes and where it is weak. So if the variation of the structure factor at the interface is not too large compared to the atomic amplitude scattering, the phase of the ideal superlattice will be preserved in the actual one, except maybe at some special k values that we can identify. One specific defect which is likely to occur, especially in the so-called 4-4 superlattice, is related to fluctuations in the superlattice period Λ . They are expected to decrease the correlations between the scattered x rays and to broaden the diffraction peaks but, in the limit of small fluctuations, they should not change the sign of the scattering amplitude.

Our simulations show that, for the $\text{Fe}_{12}/\text{Ru}_{16}$ superlat-

tice, the sign of the phases is well defined for all reflections over a large range of values of the c parameters around $d_{\text{Fe}} \sim 2.055 \text{ \AA}$ and $d_{\text{Ru}} \sim 2.165 \text{ \AA}$ (see Fig. 3), except for the phase of the low-intensity satellite at the high- k side of the (0002) peak. For this reflection, the phase obtained calculating the supercell scattering amplitude with the lattice constant found in the preceding paragraph has been used. However, its intensity is so weak that a change in its sign does not modify the Fourier transform. We have therefore calculated the FT of the square root of the measured scattered intensity for all reflections with the phase factors of a perfect crystal. This yields the profile of the electronic density across the superlattice. A translation of the origin in real space by one wavelength Λ does not change the phase (at least in the limit of a thick crystal), so what we get is the electronic distribution centered on one of the two different kinds of bilayer and averaged over the whole sample. We can, however, choose either the center of an iron or a ruthenium layer as the origin, the calculated phase factors being different in the two cases. Figure 5 shows over one period (14 atomic planes) the FT obtained from the data measured at 7112 eV, with the phases calculated for the origin in the middle of an iron layer. At all the energies we have worked with, the $f_{\text{Ru}}(E, k)$ is almost independent from E , so the difference between the Fourier transforms of data measured at two different energies eliminates Ru contribution, being the FT of $\sum_{\text{Fe}} \Delta f_{\text{Fe}}(E, k) \exp(iz_{\text{Fe}}k)$. Two determinations of the Fourier-transformed difference (FTD) obtained using sets of data taken at different energies are displayed in the lower panel of Fig. 5, the origin also having been taken in the center of a Fe layer. We can now see directly the iron distribution in each atomic plane. The first three planes are mainly Fe ones, though the amplitude of the third one at the interface with the Ru layer is somewhat re-

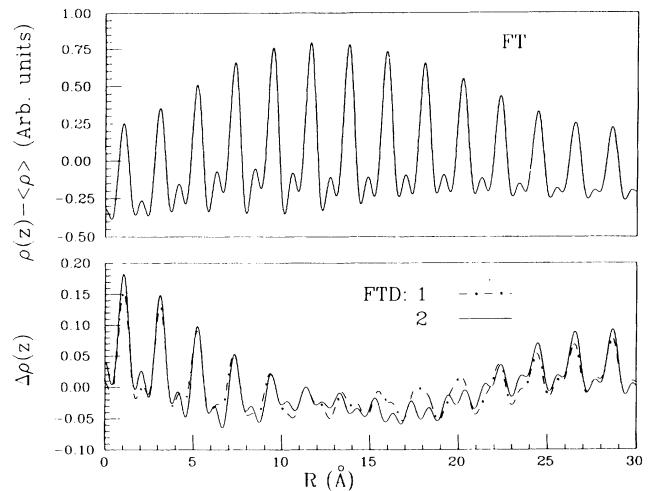


FIG. 5. Upper panel: Fourier transform of the scattered amplitude for the $\text{Fe}_{12}/\text{Ru}_{16}$ superlattice ($E = 7112 \text{ eV}$). Lower panel: Fourier-transform differences (plot 1: FT at 15203 eV minus FT at 7112 eV; plot 2: FT at 8333 eV minus FT at 7112 eV). These plots represent the iron atomic density profile.

duced suggesting some Ru diffusion. The fourth plane is clearly a mixed one, with about a half plane of iron atoms. At larger R values we find six ruthenium planes characterized in the FTD by an iron density which is almost zero, then a second interface with two mixed planes, followed by two iron planes. If we correct for Debye-Waller effects the plot is symmetric as expected around $R = \Lambda/2$ ($\Lambda = 29.65 \text{ \AA}$). A modulation of the electronic density is seen with the maximum at half period in the center of the Ru layer. On average the thickness of the iron layers is between six and seven atomic planes. Each interface between iron and ruthenium layers extends roughly over two atomic planes. At this step we cannot distinguish between interdiffusion and fluctuation of the thickness of Fe and Ru layers.

A lot of experimental problems preclude in this case a more quantitative analysis. The long-wave modulation which is found both in FT and FTD's comes from the low-angle part in the scattering pattern. It is due to inaccuracies in the correction of absorption or/and in the refraction index value which is used to rescale the k axis. Both effects are important only at low angle. The peak widths and the spurious oscillations which are the main drawbacks in this method are due to the short- k range available at the iron- k edge energy. Moreover the contributions of the Ru buffer Bragg peaks have been simulated and subtracted from the experimental spectra. Whatever the accuracy of this procedure is, it always leaves a weak crystalline Ru contribution that should, however, be erased in the FTD.

To get a good FTD it is critical to accurately normalize the spectra intensities, which has been done by using the intensity diffracted by the Ru buffer. However, we have seen that changing the normalization by about 5% allows us to eliminate in the FTD small nonphysical negative peaks at the ruthenium planes positions, without changing significantly the intensities at the iron planes positions. Such an adjustment can be justified because of the error bar on the normalization procedure which is due both to the fact that ruthenium and multilayer peaks are not fully deconvolved, and to absorption effects.

As already mentioned, we can calculate the phases by choosing the origin in real space in the middle of an iron or ruthenium layer. The best way to obtain the interplanar distances in the two sublattices is to take the position of the first peak in the FT's calculated with the two different sets of phase assignments, measuring in this way $d_{\text{Fe}}/2$ and $d_{\text{Ru}}/2$. We obtain $c_{\text{Fe}} \sim 4.12 \pm 0.02 \text{ \AA}$ and $c_{\text{Ru}} \sim 4.32 \pm 0.02 \text{ \AA}$. These values are in excellent agreement with those obtained by the simulation in k space, giving a coherent picture.

We have performed the FT analysis on a second multilayer nominally Ru_4/Fe_4 using the same method. In this case too, the simulated amplitude has a well-defined sign for each peak. In the upper panel of Fig. 6 we show the FT of the phased scattered amplitude for an experiment at the iron edge. We have chosen the phase factor so that the origin in real space is located at the center of an iron layer. We find out that the intensity ratio of the first two peaks is actually equal to that of the scattering factors of iron and ruthenium, corrected for the anomalous contri-

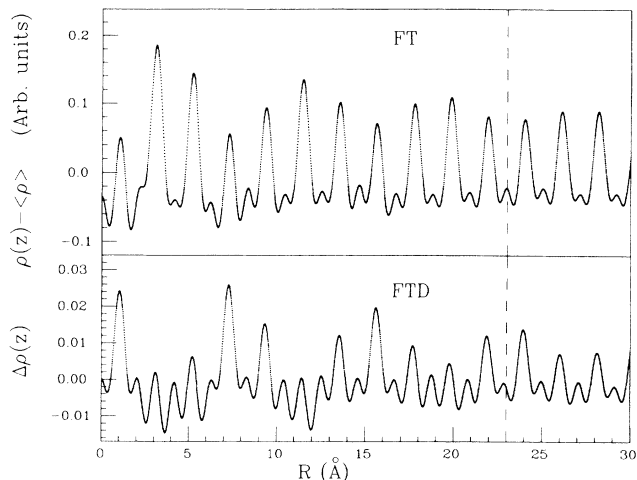


FIG. 6. Upper panel: Fourier transform of the scattered amplitude for the Fe_4/Ru_4 superlattice ($E = 7112 \text{ eV}$). Lower panel: Fourier-transform difference (FT at 7709 eV minus FT at 7112 eV).

bution. Looking at the FT plot we find a symmetry between the eleventh and the twelfth plane suggesting a superperiod of eleven atomic planes. This is coherent with the analysis of the peak positions in k space (we have a pseudoperiod of $\frac{11}{3} \sim 3.7$ planes). We can reach a deeper insight by looking at the FTD calculated from data obtained at the iron edge (7112 eV) and far from it (7709 eV), which is shown in the lower part of Fig. 6. Despite the truncation parasitic oscillations, we directly visualize the interface between iron and ruthenium which is located between the first and the second atomic plane in Fig. 6. We very clearly see how abrupt it is. Looking at the next ruthenium-iron interface (between the third and the fourth plane) we observe the presence of iron in the nominally ruthenium third plane. It cannot be due to interdiffusion since interdiffusion is not observed at the first Fe-Ru interface, but it evidences the existence of incomplete layers of ruthenium. This is in good agreement with the observation of a noninteger pseudoperiod of 3.7 atomic planes. To obtain a self-consistent result, we have recalculated the phases for a multilayer with such a period of about 3.7 atomic planes by using a superstructure of six pseudoperiods corresponding to 22 atomic planes and assuming that each pseudoperiod is constituted by two iron planes and 1.66 ruthenium ones. The phases obtained for each reflection are the same as those calculated for an ideal superlattice with a period of four atomic planes, which justifies their practical use.

CONCLUSION

We present the results of a structural study of MBE-grown iron-ruthenium superlattices by using x-ray anomalous diffraction. In this metallic superlattice iron grows on ruthenium in an hexagonal phase which is magnetic for iron layers thicker than $\sim 8 \text{ \AA}$. The aim of the present study was to try to correlate the magnetic properties to the atomic structure of the iron layers. We thus

have investigated both the iron atomic volume in the superlattice and interdiffusion at the Fe/Ru interfaces.

To do this, we have used anomalous x-ray diffraction, which allows us to selectively probe the iron layer. This capability can be exploited both directly in k space by comparing the intensity variations of simulated spectra to the measured ones, and in R space via Fourier-transform methods. By phasing the x-ray reflections we have in this case traced the electronic density along the growth direction. In this way, we have found that in Fe/Ru superlattice the interdiffusion at the interface is weak. For the short period multilayer (Fe₄/Ru₄) we find a sharp interface without significant interdiffusion. For the longer period one (Fe₁₂/Ru₁₄) it is not possible to separate the effects of interdiffusion and of the fluctuation of the thickness of the iron and ruthenium layers. However, interdiffusion occurs at most over two planes at the interface.

In the Fourier-transformed curves we have also measured directly the Fe-Fe and Ru-Ru distances. The values found agree with those obtained from the variation

of the intensities of the satellites due to anomalous scattering, though the degree of accuracy is lower.

The jointed study of anomalous x-ray diffraction in reflection geometry and of x-ray diffraction in transmission geometry allows us to evaluate the iron atomic volume. We find $V_{\text{Fe}} \sim 12.87 \text{ \AA}^3$, with an increase of about 14% compared to the high-pressure hcp phase. This large atomic volume can be achieved thanks to the constraint of the ruthenium sublattice, and explains partially the magnetic behavior of Fe/Ru superlattices. Theoretical calculations from Kübler⁴ show in fact that for this large atomic volume the ground state of bulk hcp iron is ferromagnetic.

The progress in evaporating techniques for preparing ultrathin films has made it possible to control each layer thickness on an atomic scale. This allows us to obtain samples with unusual electronic, magnetic, and transport properties. It is of primary importance to well characterize the atomic structure of the samples. We think that anomalous x-ray diffraction might become a unique tool for these kinds of studies.

*Present address: Dipartimento di Fisica dell'Università dell'Aquila, 67010 Coppito, Italy.

†Present address: Instituto de Ciencia de Materiales, Departamento de Física Aplicada, Universidad Autónoma de Madrid, 28049 Madrid, Spain.

‡Present address: Laboratoire de Cristallographie, CNRS, 38042, Grenoble, France.

§Present address: Compagnie de Saint Gobain, 92000 Courbevoie, France.

**Present address: Centre National d'Études des Télécommunications, Laboratoire de Microstructures, 92220 Bagneux, France.

¹C. Chatillon and J. Massies, in Proceedings of the Summer School on Metallic Multilayers, Aussois, France, 1989, edited by A. Chamberod and J. Hillairet [Mater. Sci. Forum **59&60**, 229 (1990)].

²C. M. Falco, J. Phys. (Paris) Colloq. **48**, C5-57 (1987).

³M. Maurer, J. C. Ousset, M. F. Ravet, and M. Piecuch, Europhys. Lett. **9**, 803 (1989).

⁴J. Kübler, Solid State Commun. **72**, 631 (1989).

⁵M. Maurer, J. C. Ousset, M. Piecuch, M. F. Ravet, and J. P. Sanchez, in *Proceedings of the Growth, Characterization, and Properties of Ultrathin Magnetic Films and Multilayers, San Diego, 1989*, MRS Symposia Proceedings No. 105 (Materials Research Society, Pittsburgh, 1989).

⁶S. Sasaki (unpublished).

⁷F. Baudalet, A. Fontaine, G. Tourillon, D. Guay, M. Maurer, M. Piecuch, M. F. Ravet, and V. Dupuis, Phys. Rev. B (to be published).

⁸Y. Fujii, T. Ohnishi, T. Ishihara, Y. Yamada, K. Kawaguchi, N. Nakayama, and T. Shinjo, J. Phys. Soc. Jpn. **55**, 251 (1986).

⁹J. M. Tonnerre, J. C. De Lima, and D. Raoux, J. Chim. Phys. **86**, 1509 (1989).